Bound states of two spin-$\frac{1}{2}$ fermions in a synthetic non-Abelian gauge field

Jayantha P. Vyasanakere* and Vijay B. Shenoy†

Centre for Condensed Matter Theory, Department of Physics, Indian Institute of Science, Bangalore 560 012, India

(Received 20 December 2010; published 11 March 2011; corrected 16 March 2011)

We study the bound states of two spin-$\frac{1}{2}$ fermions interacting via a contact attraction (characterized by a scattering length) in the singlet channel in three-dimensional space in presence of a uniform non-Abelian gauge field. The configuration of the gauge field that generates a Rashba-type spin-orbit interaction is described by three coupling parameters $(\lambda_x,\lambda_y,\lambda_z)$. For a generic gauge field configuration, the critical scattering length required for the formation of a bound state is *negative*, i.e., shifts to the "BCS side" of the resonance. Interestingly, we find that there are special high-symmetry configurations (e.g., $\lambda_x=\lambda_y=\lambda_z$) for which there is a two-body bound state for *any* scattering length however small and negative. Remarkably, the bound-state wave functions obtained for such configurations have nematic spin structure similar to those found in liquid ^{3}He. Our results show that the BCS-BEC (Bose-Einstein condensation) crossover is drastically affected by the presence of a non-Abelian gauge field. We discuss possible experimental signatures of our findings both at high and low temperatures.

DOI: 10.1103/PhysRevB.83.094515 PACS number(s): 03.65.Ge, 05.30.Fk, 67.85.−d, 71.70.Ej

I. INTRODUCTION

Quantum emulation experiments with cold quantum gases[1–3] and optical lattices hold the promise of providing clues to understanding many outstanding issues of quantum condensed matter physics such as high-temperature superconductivity, the quantum hall effect, etc., and the high-energy physics of strongly coupled gauge theories.[4] While this has led to a flurry of activity, many experimental challenges remain in the way of redemption of this promise. Particular among them are the problem of entropy removal and the creation of magnetic (gauge) fields.

Realization of magnetic fields has been achieved by rotation;[5] however, attaining magnetic fields corresponding to quantum hall regimes has serious experimental challenges. There have been many theoretical suggestions for the generation of artificial gauge fields,[6–9] both Abelian and non-Abelian. Recently Spielman and co-workers[10,11] used Raman coupling between hyperfine states to produce synthetic gauge fields. They studied Bose condensates of ^{87}Rb atoms and investigated the punching in of vortices when a U(1) gauge field corresponding to a magnetic field is tuned. Depending on the degeneracy of the lowest Raman coupled states, one can also generate non-Abelian gauge fields. The condensation of bosons in non-Abelian fields have been investigated.[12,13]

These developments provide us the motivation to study *fermions* in non-Abelian gauge fields. The simplest in this class is the case of spin-$\frac{1}{2}$ particles coupled to an SU(2) gauge field. Study of such systems within the cold atoms context will enable experimental realization and understanding of fermionic Hamiltonians with spin-orbit interactions that can lead to interesting topological phases of matter.[14,15]

Readers who wish to obtain a qualitative understanding of our work may read Sec. II where we state our problem and summarize our results, followed by Sec. V which discusses the significance of these results. Sec. III contains details of our calculations, and Sec. IV provides a qualitative discussion of the physics of our results.

II. STATEMENT OF THE PROBLEM AND SUMMARY OF RESULTS

We consider spin-$\frac{1}{2}$ fermions moving in a three-dimensional continuum in a non-Abelian gauge field. The simplest realization of this is described by the Hamiltonian

$$\mathcal{H}_{\rm GF}=\int d^3\boldsymbol{r}\,\Psi^\dagger(\boldsymbol{r})\left[\frac{1}{2}\left(p_i\mathbf{1}-A_i^\mu\boldsymbol{\tau}^\mu\right)\left(p_i\mathbf{1}-A_i^\nu\boldsymbol{\tau}^\nu\right)\right]\Psi(\boldsymbol{r}), \tag{1}$$

where $\Psi(\boldsymbol{r})=\{\psi_\sigma(\mathbf{r})\},\sigma=\uparrow,\downarrow$ is a two-component spinor field (spin quantization along z axis), p_i is the momentum operator $(i=x,y,z)$, $\mathbf{1}$ is the SU(2) identity, $\boldsymbol{\tau}^\mu$ are Pauli spin operators $(\mu=x,y,z)$, and A_i^μ describe a *uniform* gauge field. We work with units where the mass of the fermions and $\hbar$ are unity. Indeed even a uniform non-Abelian field leads to interesting physics,[12] an example of which we demonstrate in this paper.

Motivated by the recent experiments mentioned above, we consider non-Abelian gauge fields of the type $A_i^\mu=\lambda_i\delta_i^\mu$ which leads to a generalized Rashba Hamiltonian describing an anisotropic spin-orbit interaction

$$\mathcal{H}_R=\int d^3\boldsymbol{r}\Psi^\dagger(\boldsymbol{r})\left(\frac{\boldsymbol{p}^2}{2}\mathbf{1}-\boldsymbol{p}_\lambda\cdot\boldsymbol{\tau}\right)\Psi(\boldsymbol{r}),\qquad \boldsymbol{p}_\lambda=\lambda_x p_x\boldsymbol{e}_x+\lambda_y p_y\boldsymbol{e}_y+\lambda_z p_z\boldsymbol{e}_z. \tag{2}$$

Here an inconsequential constant term has been dropped. The gauge coupling strength is $\lambda=\sqrt{\lambda_x^2+\lambda_y^2+\lambda_z^2}$, and the vector $\boldsymbol{\lambda}\equiv\lambda\hat{\boldsymbol{\lambda}}=\lambda_x\boldsymbol{e}_x+\lambda_y\boldsymbol{e}_y+\lambda_z\boldsymbol{e}_z$ defines a gauge field configuration (GFC).

We now describe the interaction between fermions by a contact attraction model in the singlet channel[16]

$$\mathcal{H}_\upsilon=\frac{\upsilon}{2}\int d^3r\,S^\dagger(\boldsymbol{r})S(\boldsymbol{r}), \tag{3}$$

where $S^\dagger(\boldsymbol{r})$ is the singlet creation operator, and υ is the bare contact interaction. The theory described by the Hamiltonian $\mathcal{H}=\mathcal{H}_R+\mathcal{H}_\upsilon$ requires an ultraviolet momentum cutoff Λ.

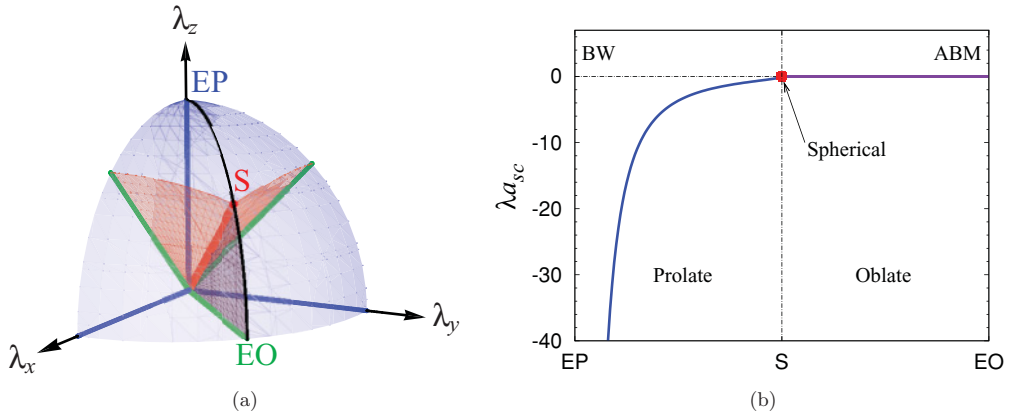

FIG. 1. (Color online) (a) Two-body phase diagram in the gauge-field configuration (GFC) space described in Eq. (2). Lines in dark blue (along the axes) correspond to extreme prolate (EP) GFCs, dark green (along 45° to the axes on the coordinate planes) correspond to extreme oblate (EO) GFCs, and the red line (along the body diagonal) corresponds to spherical (S) GFCs. The wings in violet hue correspond to oblate GFCs. For the oblate, including EO GFCs, and the S GFCs, a bound state is obtained for any scattering length i.e., $a_{sc} = 0^-$. Regions with a blue hue, including the axes (EP), correspond to GFCs that require a nonzero critical scattering length for the formation of a bound state. (b) Critical scattering length along the path EP-S-EO as shown in (a). For the EP GFCs, the symmetry of the bound-state wave function corresponds to an extended Balian-Werthamer (BW) state with a biaxial nematic spin order, while that in the EO state corresponds to an extended Anderson-Brinkman-Morel (ABM) state with a uniaxial nematic spin order. The state evolves smoothly from a biaxial nematic to a uniaxial nematic passing through the S configuration where the bound state is rotationally symmetric.

The bare contact interaction parameter υ is Λ dependent and satisfies the regularization relation $\frac{1}{\upsilon} + \Lambda = \frac{1}{4\pi a_s}$, where a_s is the s-wave scattering length in the *absence* of the gauge field ("free vacuum"). It is well known[17] that for a pair of spin-$\frac{1}{2}$ fermions in free vacuum, there is no bound state when $a_s < 0$ (conventionally called the BCS side), and a bound state develops when $1/a_s = 0$ (resonance), and for $a_s \geqslant 0$ (Bose-Einstein condensation or BEC side), the binding energy $E_b = \frac{1}{a_s^2}$. This result embodies the fact that a critical attraction, characterized by the critical scattering length a_{sc}, is needed to obtain a two-body bound state in the three-dimensional free vacuum where $1/a_{sc} = 0$.

In this paper we address the question of how a uniform gauge field described by Eq. (2) affects the nature of the bound state of two fermions interacting via Eq. (3). To this end, we obtain the "phase-diagram" of the two-fermion problem in the GFC space described by the parameters $\lambda_x, \lambda_y, \lambda_z$ of Eq. (2), by studying the bound state as a function of the free-vacuum scattering length a_s.

GFCs can be conveniently classified as being prolate when two of the λs are equal and *smaller* than the third, oblate when two of the λs are equal and *larger* than the third, spherical (S) when all three λs are equal, and generic when no two λs are equal. Our main findings are summarized in Fig. 1. We show that for prolate and generic GFCs, the critical scattering length a_{sc} required for the bound-state formation is *negative*, i.e., shifts to the BCS side. However, for oblate and spherical GFCs a_{sc} vanishes, i.e., there is a bound state for *any* scattering length [see Fig. 1(b)]. The key difference between the oblate and spherical cases is the size of the binding energy of the bound state. In the deep BCS side, for oblate gauge fields, the binding energy depends exponentially on a_s and λ, while for spherical gauge fields, an algebraic dependence is obtained. Evidently, these results of the two-body problem suggest that many-body physics of fermions, in particular, the crossover from the BCS regime to the BEC regime, will be spectacularly affected by the presence of a non-Abelian gauge field. Moreover, our results below indicate that the superfluid obtained at low temperatures will also have additional spin nematic order induced by the gauge field.

III. TWO-BODY PROBLEM IN PRESENCE OF NON-ABELIAN GAUGE FIELDS

For any GFC, the single-particle states are described by the quantum numbers of momentum $\boldsymbol{k}$ and helicity α (which takes on values $\pm$):

$$|\boldsymbol{k}\alpha\rangle = |\boldsymbol{k}\rangle \otimes |\alpha\hat{\boldsymbol{k}}_\lambda\rangle, \tag{4}$$

where $|\boldsymbol{k}\rangle$ is the usual plane-wave state, and $|\alpha\hat{\boldsymbol{k}}_\lambda\rangle$ is the spin-coherent state in the direction $\alpha\hat{\boldsymbol{k}}_\lambda$, with $\boldsymbol{k}_\lambda$ defined analogous to $\boldsymbol{p}_\lambda$ of Eq. (2). The two helicity bands disperse as

$$\varepsilon_{\boldsymbol{k}\alpha} = \frac{k^2}{2} - \alpha|\boldsymbol{k}_\lambda|. \tag{5}$$

The full two-body Hamiltonian $\mathcal{H}$ generically has only two symmetries: global translation and time reversal. Therefore, the only good quantum number is the center of mass momentum of the two particles. We shall focus attention on states with zero center of mass momentum, and perform a T-matrix analysis[17] in the relative-momentum and helicity bases. The components of the T matrix have the matrix structure $T_{\beta\beta'}(\omega)$, where ω is the energy, and β, β' run over $(++, +-, -+, --)$, the helicity indices of the two fermions. Since the interaction is only in the singlet channel, it follows that components with indices $(+-, -+)$ vanish. This analysis, along with the regularization discussed earlier, readily provides the condition for bound-state formation

$$\frac{1}{4\pi a_s} = \frac{1}{2V}\sum_{\boldsymbol{k}\alpha}\left(\frac{1}{E - 2\varepsilon_{\boldsymbol{k}\alpha}} + \frac{1}{k^2}\right), \tag{6}$$

where V is the volume of space under consideration. Isolated poles of the T matrix, which correspond to bound states, are obtained by finding the roots E of Eq. (6). We shall now present results for particular GFCs including the nature of the bound-state wave functions.

A. Extreme prolate (EP)

In EP GFCs, two of the gauge couplings vanish (say, $\lambda_x = \lambda_y = 0$), while only one is nonzero ($\lambda_z = \lambda$). Such configurations correspond to the axes marked in blue (along the axes) in Fig. 1(a). These GFCs possess, in addition to translation and time reversal, spatial and spin rotation symmetries about the z axis. The one-particle dispersion (5), for this case, provides the scattering threshold $E_{\rm th} = -\lambda^2$. Defining the binding energy $E_b = -(E - E_{\rm th})$, we find from the solution of Eq. (6) that a bound state appears only for positive scattering lengths (Fig. 2), with

$$E_b = \frac{1}{a_s^2}, \quad a_s > 0. \tag{7}$$

The critical scattering length corresponds to resonance, i.e., $1/a_{\rm sc} = 0$.

These results for E_b and $a_{\rm sc}$ are identical to those of the two-body problem in free vacuum. There is, however, a crucial difference. The wave function of the bound state in the absence of the gauge field is a spin singlet. In an extreme prolate gauge field, the bound-state wave function has two pieces,

$$\Psi_b \propto \psi_s(\boldsymbol{r})|\uparrow\downarrow - \downarrow\uparrow\rangle + \psi_a(\boldsymbol{r})|\uparrow\downarrow + \downarrow\uparrow\rangle, \tag{8}$$

where $\psi_s(\boldsymbol{r}) = \sum_{k\alpha} \frac{\cos k\cdot r}{2\varepsilon_{k\alpha} - E}$ and $\psi_a(\boldsymbol{r}) = \sum_{\boldsymbol{k}\alpha} \frac{\alpha \sin k\cdot r}{2\varepsilon_{k\alpha} - E}$ are, respectively, symmetric and antisymmetric functions of the relative coordinate $\boldsymbol{r}$. The first piece is a spin singlet, while the second piece (which vanishes when $\lambda \to 0$) has a triplet spin wave function. This wave function corresponds to an extended BW state[18] of the B-phase of ^{3}He with an additional singlet piece. This state has a spin-nematic order[19] corresponding to a *biaxial nematic*, consistent with the symmetries of the Hamiltonian.

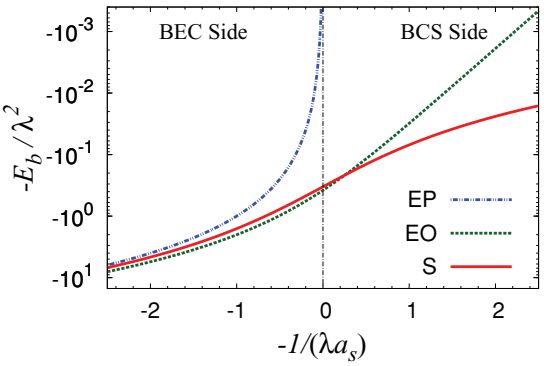

FIG. 2. (Color online) Binding energy E_b as a function of the scattering length a_s for extreme prolate (EP), extreme oblate (EO) and spherical (S) gauge field configurations. In the EP case, a bound state is obtained only for $1/a_s \geqslant 0$, while for the other two it is obtained for every a_s. In the BCS side, E_b depends exponentially on λa_s for the EO configurations, while it is a power law in the S case.

B. Extreme oblate (EO)

The EO configurations have one of the gauge couplings equal to zero and the other two equal and nonzero, and they are marked by green lines (lines at 45° to the axes on the coordinate planes) in Fig. 1. We consider the case with $\lambda_x = \lambda_y = \frac{\lambda}{\sqrt{2}}, \lambda_z = 0$. For EO GFCs, we have in addition to translation and time reversal, a symmetry of global (spatial + spin) rotation about the z axis generated by $J_z = L_z + \frac{1}{2}\tau_z$, where L_z is the z component of the orbital angular momentum operator. The solution of Eq. (6) provides an interesting result: there is a bound state for *any* scattering length, negative or positive, i.e., $a_{\rm sc} = 0^-$. For small negative a_s (BCS regime), we obtain the binding energy (with respect to the scattering threshold $E_{\rm th} = -\frac{\lambda^2}{2}$) as

$$\frac{E_b}{\lambda^2} = \sum_{n=0}^{\infty} (-1)^n a_n \left(\frac{4}{e^2} e^{\frac{-2\sqrt{2}}{\lambda|a_s|}}\right)^{n+1} \approx \frac{4}{e^2} e^{\frac{-2\sqrt{2}}{\lambda|a_s|}}, \tag{9}$$

where a_n are positive rationals tending asymptotically to $(4e)^{\frac{n}{2}}$; $a_0 = 1; a_1 = 1; a_2 = \frac{7}{4}; a_3 = \frac{23}{6}$. Thus the binding energy is exponentially small for small negative a_s. For small positive a_s (BEC regime), we have

$$\frac{E_b}{\lambda^2} = \frac{1}{(\lambda a_s)^2} + \frac{\log 2}{\sqrt{2}\lambda a_s} + \frac{4 + \log^2 2}{8} - \frac{(\lambda a_s)^2}{12} + \cdots, \tag{10}$$

which recovers the binding energy of $1/a_s^2$ in the limit of free vacuum ($\lambda \to 0$). When $1/a_s = 0$ (resonance), the binding energy is determined solely by λ; we obtain, near resonance,

$$\frac{E_b}{\lambda^2} = \mathcal{C} + \frac{2\sqrt{2}\mathcal{C}}{\sqrt{1+2\mathcal{C}}} \frac{1}{\lambda a_s} + \frac{4\mathcal{C}(1+\mathcal{C})}{(1+2\mathcal{C})^2} \frac{1}{(\lambda a_s)^2} + \cdots, \tag{11}$$

where $\mathcal{C} \approx 0.381$. The full evolution of the bound-state energy as a function of the scattering length a_s is shown in Fig. 2.

The bound-state wave function, again, has two pieces

$$\Psi_b \propto \psi_s(\boldsymbol{r})|\uparrow\downarrow - \downarrow\uparrow\rangle + \psi_a(\boldsymbol{r})|\uparrow\uparrow\rangle + \psi_a^*(\boldsymbol{r})|\downarrow\downarrow\rangle, \tag{12}$$

where $\psi_s(\boldsymbol{r}) = -\sum_{k\alpha} \frac{\cos k\cdot r}{2\varepsilon_{k\alpha} - E}$, and $\psi_a(\boldsymbol{r}) = i \sum_{k\alpha} \frac{\alpha e^{-i\phi_k} \sin k\cdot r}{2\varepsilon_{k\alpha} - E}$, $\phi_{\boldsymbol{k}}$ is the angle made by $k_x \boldsymbol{e}_x + k_y \boldsymbol{e}_y$ with the x axis. The first piece is orbitally symmetric $[\psi_s(\boldsymbol{r})]$ spin singlet (the first term), and the second piece (next two terms) consists of an antisymmetric orbital wave function $[\psi_a(\boldsymbol{r})]$ and a spin structure corresponding to that of the ABM state[18] in the A-phase of ^{3}He. This state has *uniaxial nematic* order.

C. Spherical (S)

This most symmetric GFC is characterized by $\lambda_x = \lambda_y = \lambda_z = \frac{\lambda}{\sqrt{3}}$ and marked by the red line (along the body diagonal) in Fig. 1(a). Apart from translation and time reversal, the S GFC has global rotational symmetries about all three axes generated by $J_i = L_i + \frac{1}{2}\tau_i$. Again, we find that a two-body bound state appears for *any* scattering length, i.e., $a_{\rm sc} = 0^-$. Also, we obtain a closed-form expression for the binding

energy (referred to the scattering threshold $E_{\rm th} = -\frac{\lambda^2}{3}$) for any scattering length

$$E_b = \frac{1}{4}\left(\frac{1}{a_s} + \sqrt{\frac{1}{a_s^2} + \frac{4\lambda^2}{3}}\right)^2. \tag{13}$$

An interesting aspect of this result is that, for a small negative scattering length (BCS side), the bound-state energy depends *algebraically* on a_s and λ,

$$\frac{E_b}{\lambda^2} \approx \left(\frac{\lambda a_s}{3}\right)^2, \tag{14}$$

i.e., a deeper bound state than the EP case is obtained (see Fig. 2) in this case. For small positive a_s, the leading term in the binding energy is that in the free vacuum. The bound state is a J singlet and has the wave function

$$\Psi_b(\boldsymbol{r}) \propto \frac{e^{-\sqrt{E_b}r}}{r}\left(\frac{\lambda}{\sqrt{3E_b}}\sin\frac{\lambda r}{\sqrt{3}} + \cos\frac{\lambda r}{\sqrt{3}}\right)|\uparrow\downarrow - \downarrow\uparrow\rangle + i\left[\left(\sqrt{E_b} + \frac{1}{r}\right)\sin\frac{\lambda r}{\sqrt{3}} - \frac{\lambda}{\sqrt{3}}\cos\frac{\lambda r}{\sqrt{3}}\right] \times \frac{e^{-\sqrt{E_b}r}}{\sqrt{E_b}r}|\uparrow\downarrow + \downarrow\uparrow\rangle_{\hat{\boldsymbol{r}}},$$

where the subscript $\hat{\boldsymbol{r}}$ on the second term indicates that the spin quantization axis is along $\hat{\boldsymbol{r}}$. The wave function is made of two pieces. The first piece corresponds to a $J = 0$ state constructed out of the $L = 0$ orbital state and a spin singlet, while the second piece is a $J = 0$ state obtained by fusing an $L = 1$ orbital state and a spin triplet state. Furthermore, orbital wave functions of both pieces are nonmonotonic, i.e., they have spatial oscillations. This is because of the existence of two length scales determined by E_b and λ. While the former dictates the exponential decay of the wave function, the latter determines the period of its spatial oscillation. This observation also applies to the wave functions discussed above for the EP and EO cases.

It is interesting to note how the bound state evolves as we go from the EP to the EO GFC along the path in GFC space indicated in Fig. 1(a). The prolate side of the path, which has a biaxial nematic order, is separated from the oblate side with a uniaxial nematic order by the spherical configuration. For the spherical configuration the bound state is fully (spatial + spin) rotationally symmetric.

D. Generic GFC

For a generic GFC, the critical scattering length for the formation of a bound state can be expressed as

$$\lambda a_{\rm sc} = \mathcal{F}(\hat{\boldsymbol{\lambda}}), \tag{15}$$

where $\mathcal{F}$ is a dimensionless number-valued function of the unit vector $\hat{\boldsymbol{\lambda}}$. The function $\mathcal{F}$ has to be obtained numerically. We find that $\mathcal{F}$ is a nonpositive function, i.e., for a generic GFC, the critical scattering length is *negative*, i.e., on the BCS side of the resonance. In other words, the strength of the critical attraction required to produce a two-body bound state is reduced by the presence of a generic gauge field. Figure 1(b) shows the evolution of $a_{\rm sc}$ along the great circle connecting the EP state to the EO state for a fixed gauge coupling, illustrating that prolate GFC has a negative $a_{\rm sc}$, while any oblate GFC has a vanishing $a_{\rm sc}$. In summary, the two-body bound state appears at resonance ($1/a_{\rm sc} = 0$) for EP GFCs marked by the blue lines (along the axes) in Fig. 1(a). For spherical GFCs marked by the red line (along the body diagonal) and for oblate GFCs marked by the planes bounded by the green (including EO) lines (along 45° to the axes on the coordinate planes) and the red line (along the body diagonal), $a_{\rm sc}$ vanishes, i.e., any attractive interaction, however small, will force a bound state for the two-body problem.

IV. QUALITATIVE DISCUSSION

We now discuss the physics behind these results. In the free vacuum, a renormalization group analysis of the field theory of the two-body problem with the contact interaction[20,21] provides two fixed points. The first is a stable one at $\upsilon_F^* = 0$ describing two free fermions, and the second, an unstable one $\upsilon_R^* = -1$ (in suitably chosen units) corresponding to the resonance; see Fig. 3. In free vacuum, a contact interaction parameter υ near υ_F^* flows toward υ_F^* and hence has similar physics as two free fermions. This corresponds to the fact that sufficiently strong attraction is required ($\upsilon < -1$) to produce a bound state. Consider now a situation with a υ near υ_F^* and a nonvanishing spherical gauge field with a coupling strength λ. We see immediately that the Rashba term described by the coupling λ is a relevant operator and the flow takes the system *away* from the free fixed point (see Fig. 3) suggesting that even a small λ has a drastic effect on a system near the free fixed point.

A deeper understanding can be obtained by considering the density of states $g(\varepsilon)$ of a single fermion moving in a gauge field, since it determines the density of states of two non-interacting fermions with zero center of mass momentum. One can easily obtain analytical expressions for the density of states for the high-symmetry GFCs. The gist of those formulas is that near the scattering threshold, for the high-symmetry GFCs discussed above,

$$g(\varepsilon) \sim \begin{cases} \sqrt{\varepsilon} & \text{for EP,} \\ \lambda(\text{constant}) & \text{for EO,} \\ \frac{1}{\sqrt{\varepsilon}} & \text{for S.} \end{cases} \tag{16}$$

In all three cases $g(\varepsilon) \to \sqrt{\varepsilon}$ as $\varepsilon \to \infty$. It is therefore clear that the infrared behavior of the density of states is behind the results presented hitherto. This motivates us to construct a

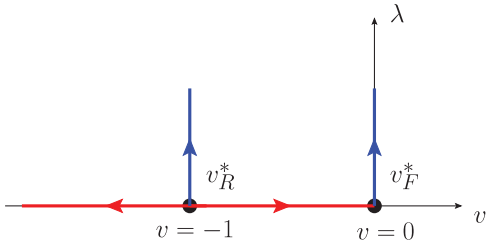

FIG. 3. (Color online) Renormalization group flow diagram (schematic) of the two-body problem. The point υ_F^* corresponds to the free fixed point and υ_R^* to resonance in vacuum.[20,21] The non-Abelian gauge field is a relevant operator at these fixed points as indicated.

model with density of states given by

$$g(\varepsilon) = \begin{cases} \frac{\sqrt{2\varepsilon_0}}{\pi^2}\left(\frac{\varepsilon}{\varepsilon_0}\right)^{\gamma}\Theta(\varepsilon) & \text{if } \varepsilon < \varepsilon_0, \\ \frac{\sqrt{2\varepsilon}}{\pi^2} & \text{if } \varepsilon \geqslant \varepsilon_0, \end{cases} \tag{17}$$

where Θ is the unit step function, γ is an exponent that determines the infrared behavior of g, and ε_0 is an energy scale (crudely equal to λ^2) at which the density of states is restored to that in the free vacuum. Note that $\gamma = \frac{1}{2}, 0, -\frac{1}{2}$ qualitatively reproduces, respectively, the density of states corresponding to EP, EO, and S GFCs. We can readily calculate the critical scattering length that obtains a bound state as

$$\sqrt{2\varepsilon_0}a_{\rm sc} = \frac{\pi\gamma}{2\gamma - 1}\Theta(\gamma). \tag{18}$$

We see immediately that $a_{\rm sc}$ vanishes whenever γ is non-positive as is the case for the EO and S configurations. For the EP configuration, the critical scattering length $a_{\rm sc} \to -\infty$ consistent with the results presented earlier. For a generic GFC, the infrared density of states has a narrow $\sqrt{\varepsilon}$ regime, followed by a regime with nearly constant density of states; this can be modeled in this simple picture using a γ that satisfies $0 < \gamma < \frac{1}{2}$, the precise value of γ being dependent on the direction $\hat{\boldsymbol{\lambda}}$ in the GFC space. We find that $a_{\rm sc}$ is negative, again, consistent with our calculations.

This simple analysis allows us to uncover the physics behind the phase diagram of Fig. 1. Highly symmetric GFCs drastically modify the low energy density of states owing to the degeneracies induced in the resulting one-particle levels. It is in this sense that the Rashba term is a relevant operator as mentioned in the discussion above. For highly symmetric GFCs, the enhanced density of states at low energies strongly promotes bound-state formation in the presence of an attractive interaction.

The particular type of nematic spin symmetry in the bound state arises so as to optimize the kinetic energy. The spin-orbit interaction mixes the singlet and triplet sectors of the two-particle system, and the particular nematic symmetry obtained in the bound state enables the orbital wave function to sufficiently "sample" the attractive interaction at a minimal cost in kinetic energy.

V. EXPERIMENTAL DIRECTIONS AND OUTLOOK

Our predictions can be readily tested by experiment. A clear signature of the bound-state formation can be obtained from the measurement of energy[22] of the gas at high temperatures. As suggested by Ho and Muller,[22] a large value of the second virial coefficient which characterizes the interaction energy is obtained for an interacting Fermi gas in free vacuum near resonance. Our results suggest that in the presence of a generic gauge field, such large corrections to energy can be observed on the *BCS side*, i.e., for negative scattering lengths near $a_{\rm sc}$ at the onset of the bound state. The quantitative value of $a_{\rm sc}$ will be affected also by the attraction in the triplet channel, but our predictions can be tested qualitatively.

Our results suggest that the BCS-BEC crossover in the presence of a non-Abelian gauge field will be drastically altered and in particular the "crossover regime" should shift to the BCS side for a generic GFC. There are many other novel effects of the non-Abelian gauge field in the many-body context such as transition in the topology of the Fermi surface with increasing filling.[23] Moreover, the two-body bound-state wave functions provide a clue to the nature of the Cooper pair wave functions. Clearly, this will lead to superfluid states with interesting pairing wave functions (such as the extended BW and ABM states found here with associated nematic orders) and concomitant excitations.

The simple model we have presented in Sec. IV suggests that our conclusions will also apply to systems with a larger gauge group, such as SU(N). Investigations along these lines should lead to interesting new possibilities with cold atom systems.

ACKNOWLEDGMENTS

Support of this work by CSIR, India (J.P.V., via a JRF grant), DST, India (V.B.S., via a Ramanujan grant), and DAE, India (V.B.S., via an SRC grant) is gratefully acknowledged. V.B.S. thanks Tin-Lun (Jason) Ho for many illuminating comments and fruitful suggestions, and Shizhong Zhang for discussions. V.B.S. expresses his gratitude to Hui Zhai for hosting a visit to Tshinghua University.

*jayantha@physics.iisc.ernet.in
†shenoy@physics.iisc.ernet.in

[1] W. Ketterle and M. W. Zwierlein, e-print arXiv:0801.2500.
[2] I. Bloch, J. Dalibard, and W. Zwerger, Rev. Mod. Phys. **80**, 885 (2008).
[3] S. Giorgini, L. P. Pitaevskii, and S. Stringari, Rev. Mod. Phys. **80**, 1215 (2008).
[4] K. Maeda, G. Baym, and T. Hatsuda, Phys. Rev. Lett. **103**, 085301 (2009).
[5] N. R. Cooper, Adv. Phys. **57**, 539 (2008).
[6] D. Jaksch and P. Zoller, New J. Phys. **5**, 56 (2003).
[7] K. Osterloh, M. Baig, L. Santos, P. Zoller, and M. Lewenstein, Phys. Rev. Lett. **95**, 010403 (2005).
[8] J. Ruseckas, G. Juzeliūnas, P. Öhberg, and M. Fleischhauer, Phys. Rev. Lett. **95**, 010404 (2005).
[9] F. Gerbier and J. Dalibard, New J. Phys. **12**, 033007 (2010).
[10] Y.-J. Lin, R. L. Compton, A. R. Perry, W. D. Phillips, J. V. Porto, and I. B. Spielman, Phys. Rev. Lett. **102**, 130401 (2009).
[11] Y.-J. Lin, R. L. Compton, K. Jimenez-Garcia, J. V. Porto, and I. B. Spielman, Nature (London) **462**, 628 (2009).
[12] T.-L. Ho and S. Zhang, e-print arXiv:1007.0650.
[13] C. Wang, C. Gao, C.-M. Jian, and H. Zhai, Phys. Rev. Lett. **105**, 160403 (2010).
[14] X.-L. Qi and S.-C. Zhang, Phys. Today , 33 (2010).
[15] M. Z. Hasan and C. L. Kane, Rev. Mod. Phys. **82**, 3045 (2010).

[16]C. J. Pethick and H. Smith, *Bose-Einstein Condensation in Dilute Gases* (Cambridge University, Cambridge, England, 2004).
[17]J. R. Taylor, *Scattering Theory* (Dover, New York, 2006).
[18]A. J. Leggett, *Quantum Liquids: Bose Condensation and Cooper Pairing in Condensed-Matter Systems* (Oxford University, Oxford, 2006).
[19]D. Podolsky and E. Demler, New J. Phys. **7** (2005).
[20]F. Sauli and P. Kopietz, Phys. Rev. B **74**, 193106 (2006).
[21]P. Nikolić and S. Sachdev, Phys. Rev. A **75**, 033608 (2007).
[22]T.-L. Ho and E. J. Mueller, Phys. Rev. Lett. **92**, 160404 (2004).
[23]J. P. Vyasanakere, S. Zhang, and V. B. Shenoy (unpublished).